Supporting information for

Remarkably improved oxygen evolution reaction activity of cobalt oxides by Fe ion solution immersion process

Shencheng Pan[1], Xin Mao[2], Juan Yu[1], Lin Hao[5], Aijun Du[2], Bing Li[1,3,4,5,*]

1. *School of Physics and Electronic Information, Huaibei Normal University, Huaibei 235000, P. R. China*
2. *School of Chemistry and Physics and Center for Material Science, Queensland University of Technology, Gardens Point Campus, Brisbane, QLD 4001, Australia*
3. *Anhui Province Key Laboratory of Pollutant Sensitive Materials and Environmental Remediation, Huaibei Normal University, Huaibei 235000, P. R. China*
4. *Information College, Huaibei Normal University，Huaibei 235000, P. R. China*
5. *Department of Physics and Astronomy, University of Tennessee, Knoxville, Tennessee 37996, USA*

* Corresponding author. E-mail: binglir@mail.ustc.edu.cn

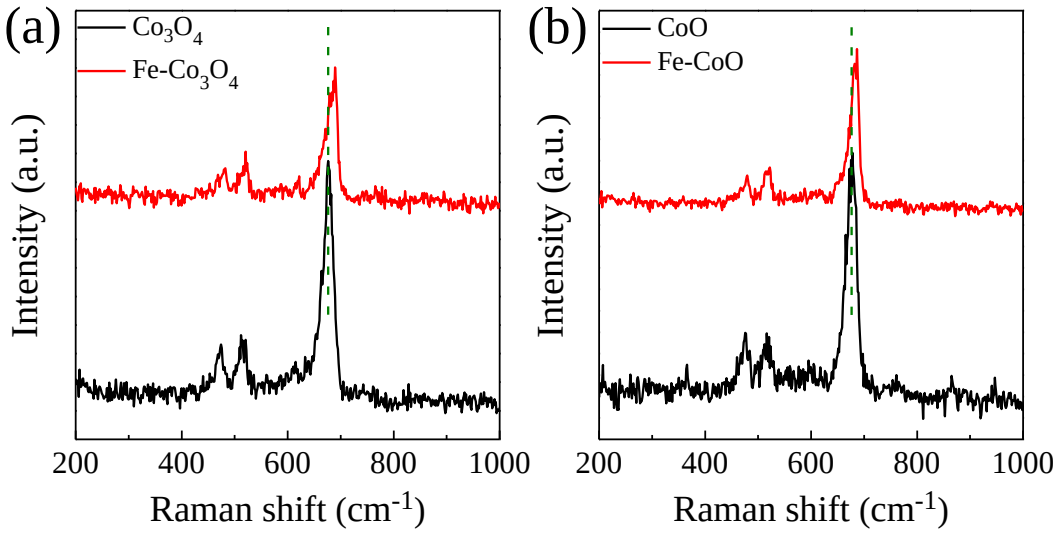

Fig. S1. Raman spectra of Co_3O_4, CoO, Fe-Co_3O_4 and Fe-CoO.

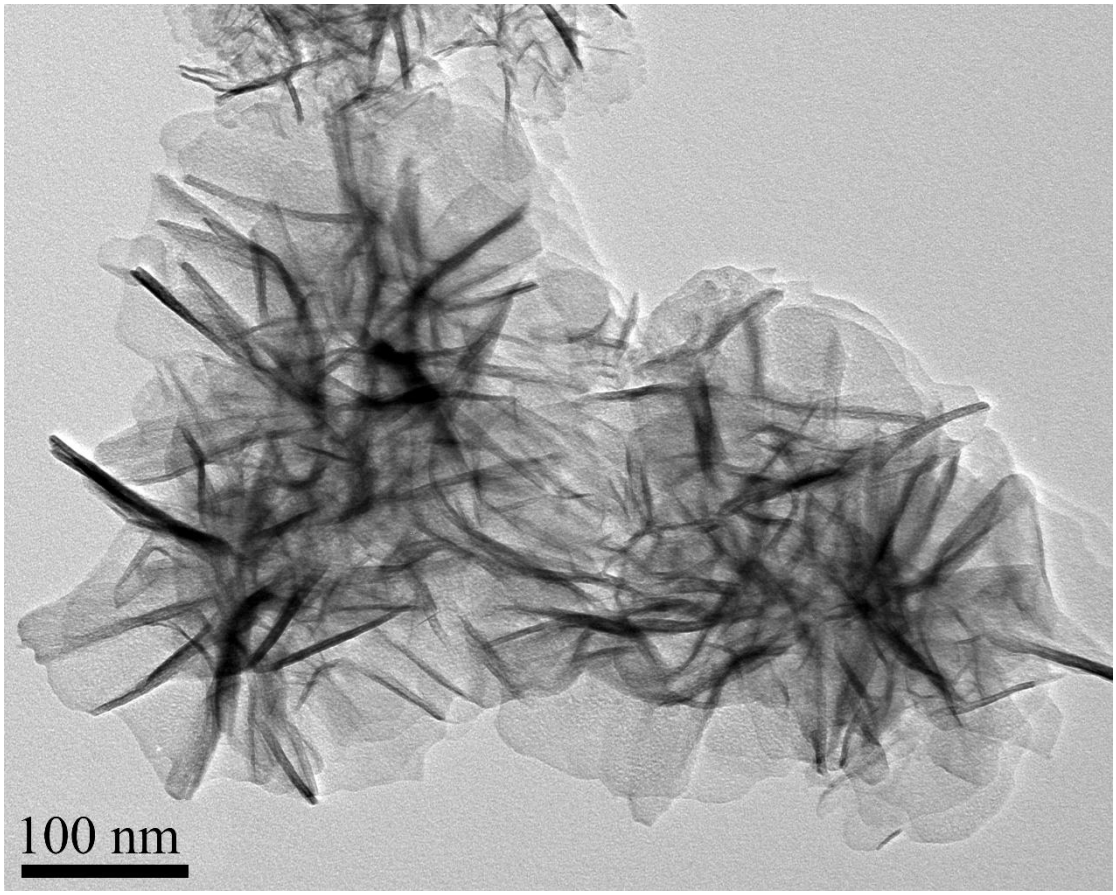

Fig. S2. TEM images of α-$Co(OH)_2$ nanoflower.

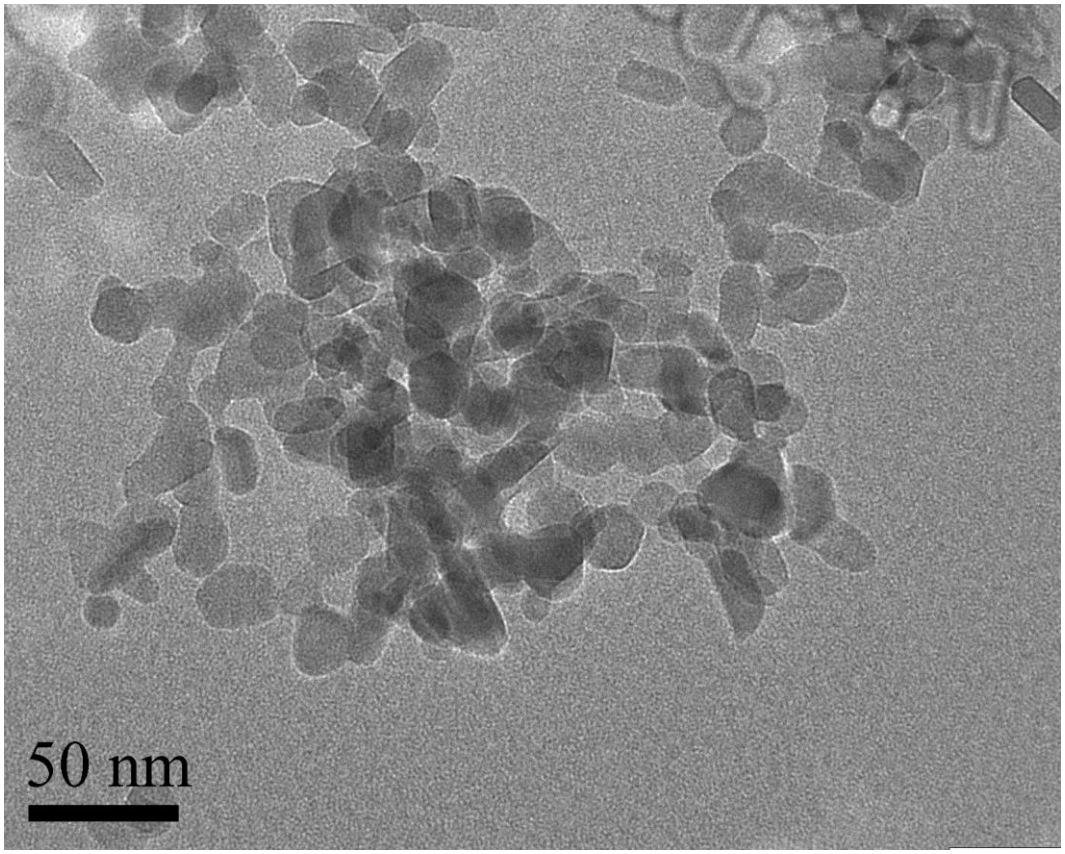

Fig. S3. TEM images of Co_3O_4 nanoparticles before Fe ion treatments.

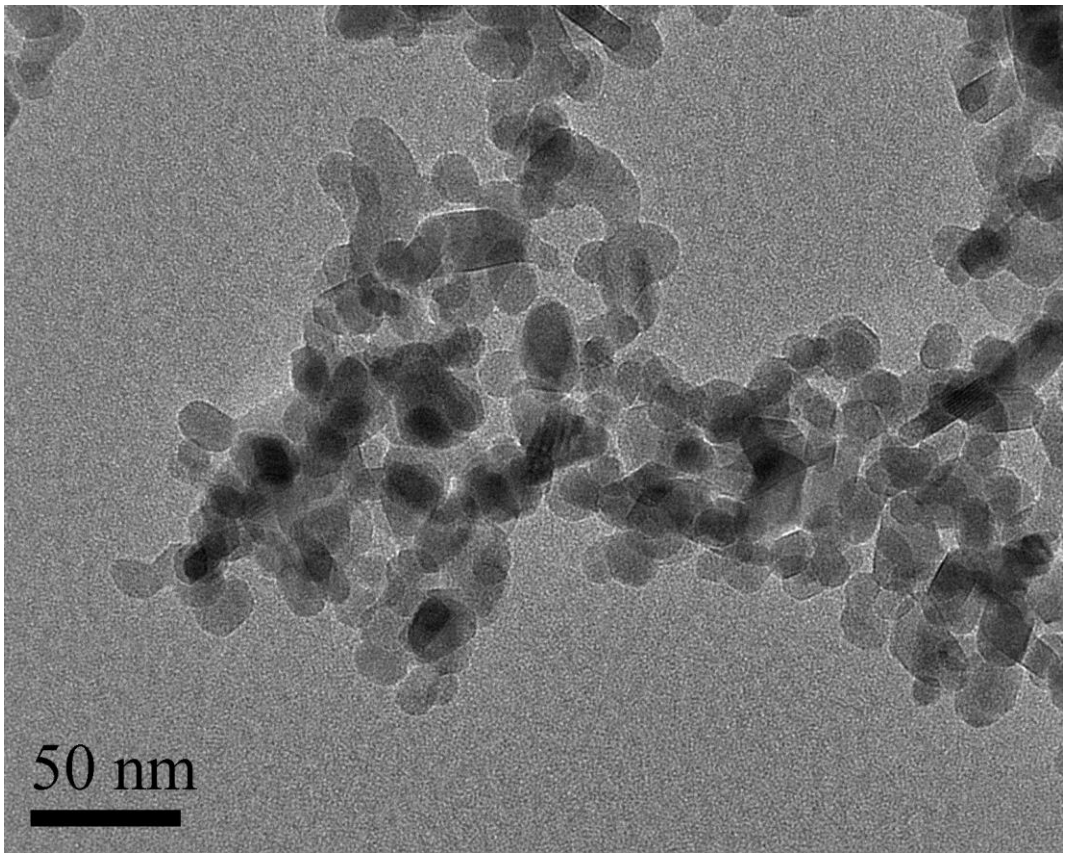

Fig. S4. TEM images of CoO nanoparticles before Fe ion treatments.

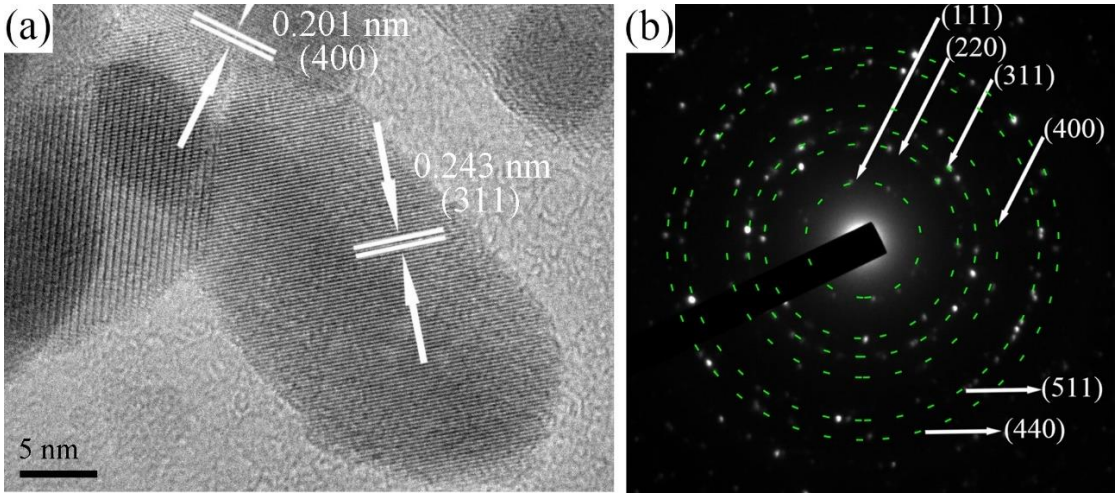

Fig. S5. (a) High resolution TEM images of Fe-Co_3O_4, (b) the SAED pattern of Fe-Co_3O_4.

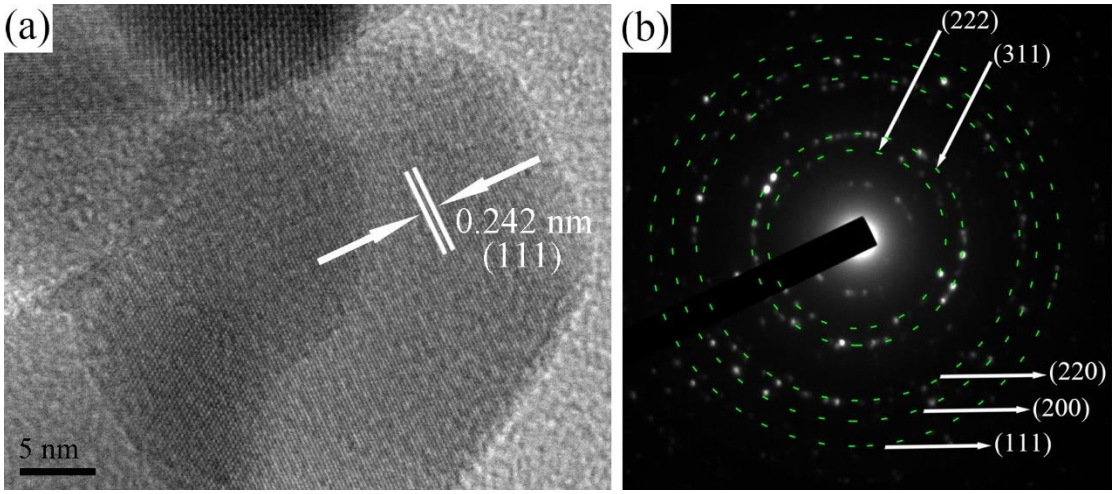

Fig. S6. (a) High resolution TEM images of Fe-CoO, (b) the SAED pattern of Fe-CoO.

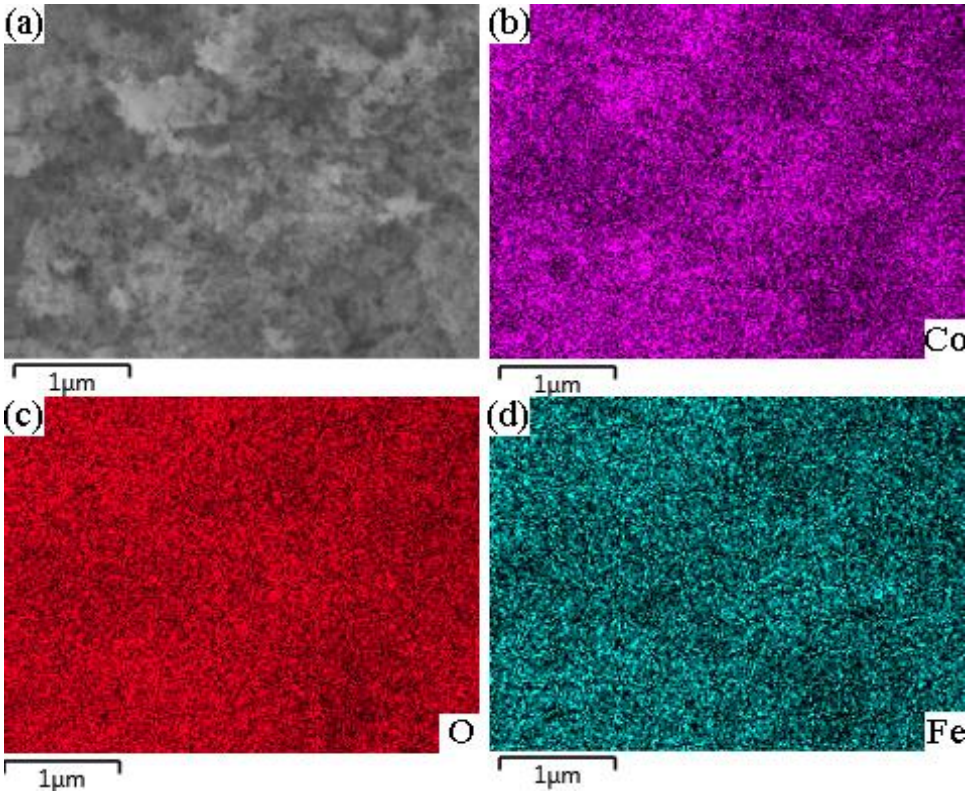

Fig. S7. SEM image (a), elemental mapping of Co (b), O (c) and Fe (d) element in Fe-Co_3O_4.

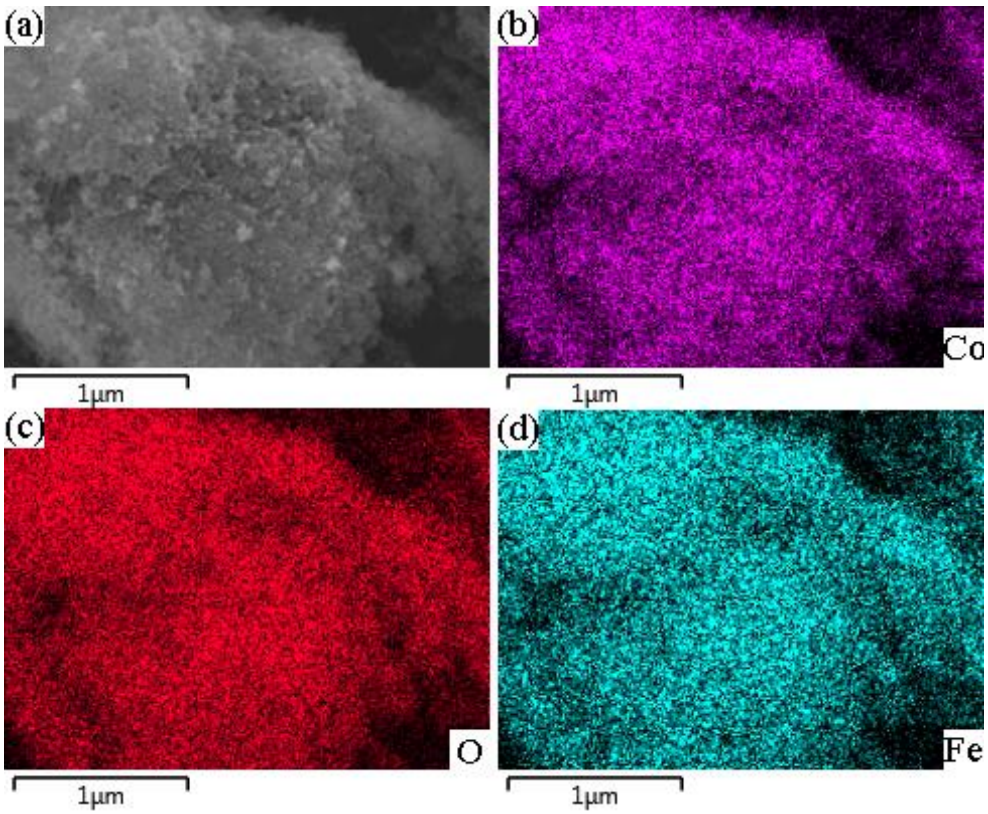

Fig. S8. SEM image (a), elemental mapping of Co (b), O (c) and Fe (d) element in Fe-CoO.

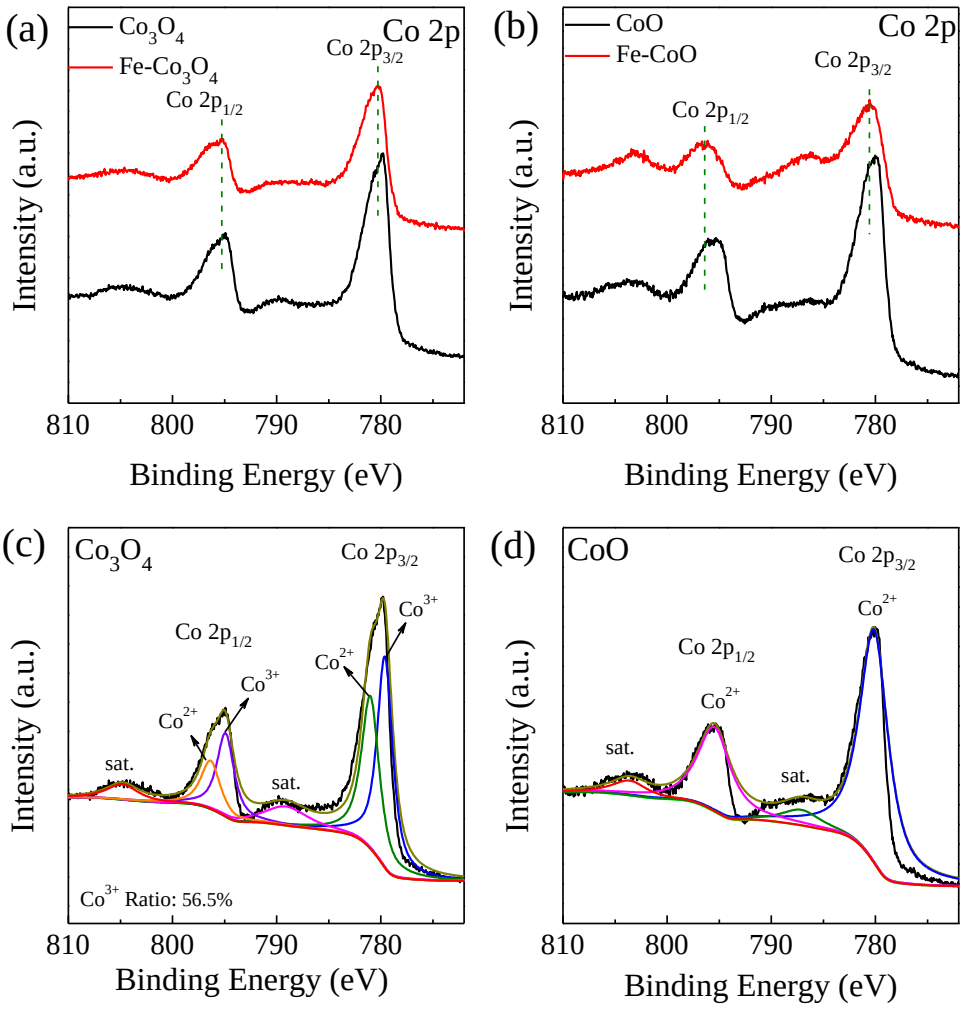

Fig. S9. (a) High resolution XPS spectrum of Co_3O_4 and Fe-Co_3O_4. (b) High resolution XPS spectrum of CoO and Fe-CoO. (c) Fitting of Co 2p XPS spectrum for Co_3O_4, (d) fitting of Co 2p XPS spectrum for CoO.

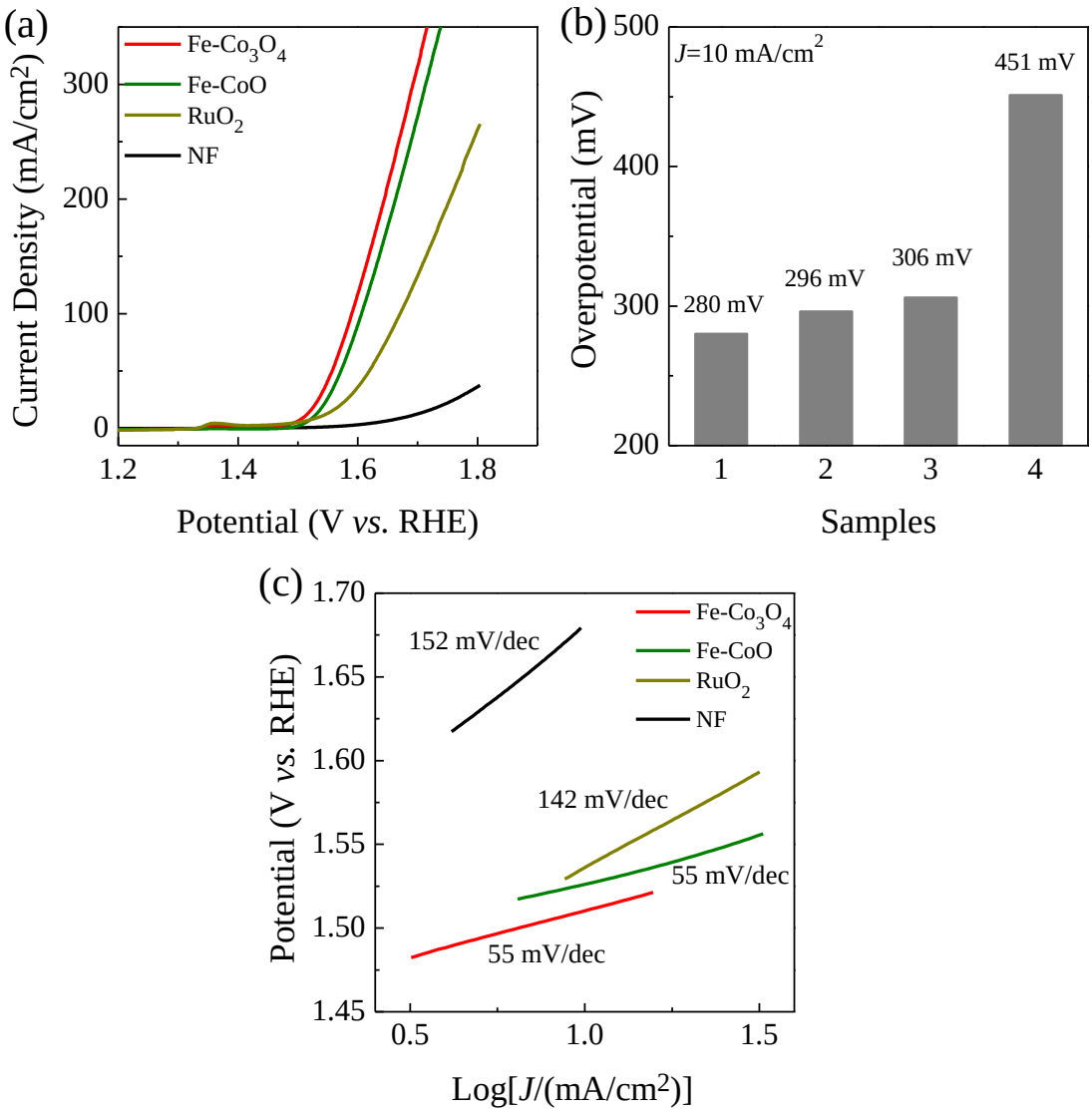

Fig. S10. (a) LSV curves of Fe-Co_3O_4, Fe-CoO, RuO_2 and no-load Ni foam. (b) Overpotential comparison histogram of Fe-Co_3O_4, Fe-CoO, RuO_2 and no-load Ni foam at a current density of 10 mA/cm^2. (c) Corresponding Tafel plots of the four prepared catalysts.

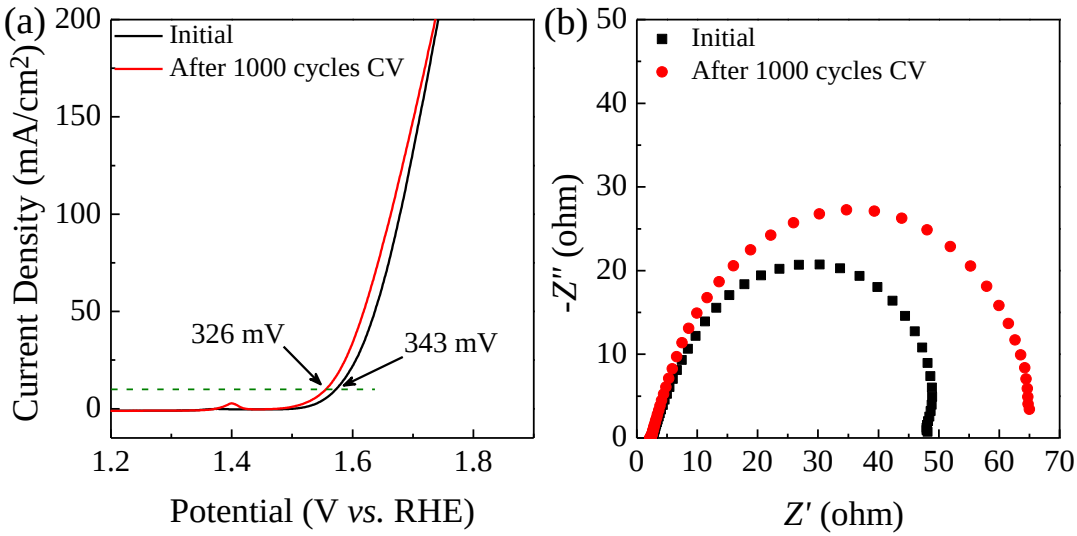

Fig. S11. Electrochemical testing of Fe-Co_3O_4 while the immersion concentration is 0.01 M (a) LSV curves, (b) Nyquist plots with an initial and after 1000 cycles CV test.

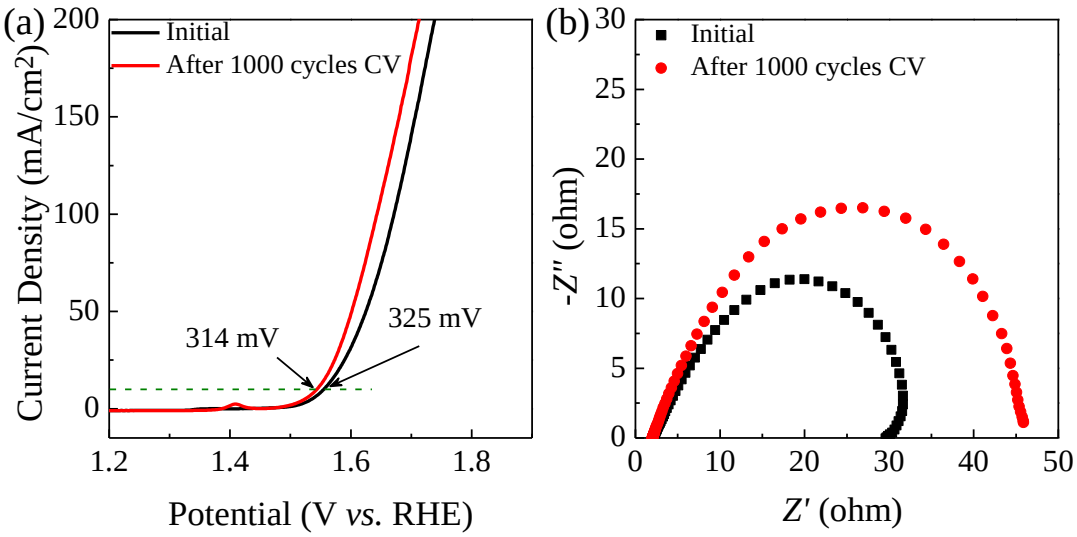

Fig. S12. Electrochemical testing of Fe-Co_3O_4 while the immersion concentration is 0.03 M (a) LSV curves, (b) Nyquist plots with an initial and after 1000 cycles CV test.

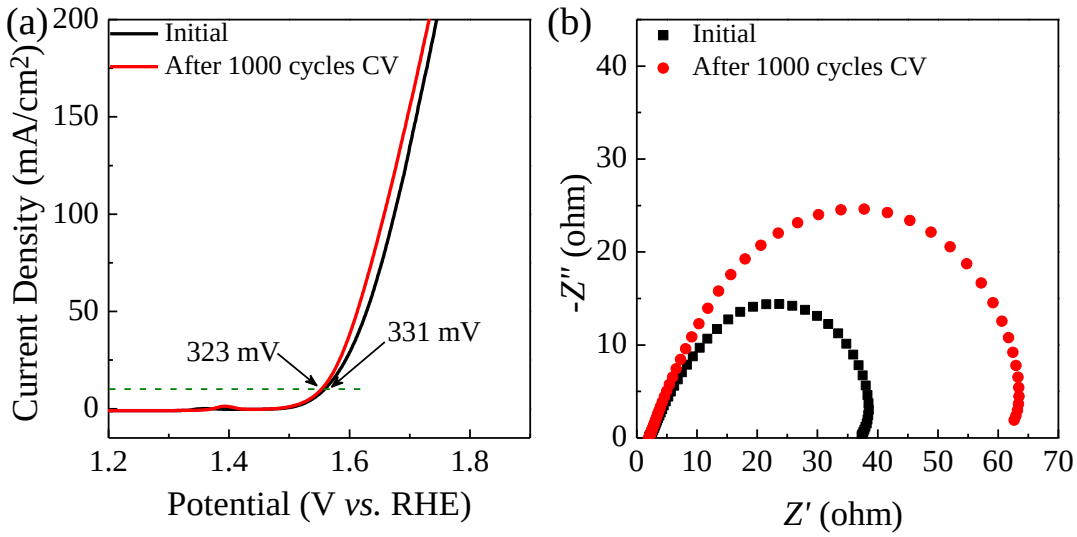

Fig. S13. Electrochemical testing of Fe-Co_3O_4 while the immersion concentration is 0.04 M (a) LSV curves, (b) Nyquist plots with an initial and after 1000 cycles CV test.

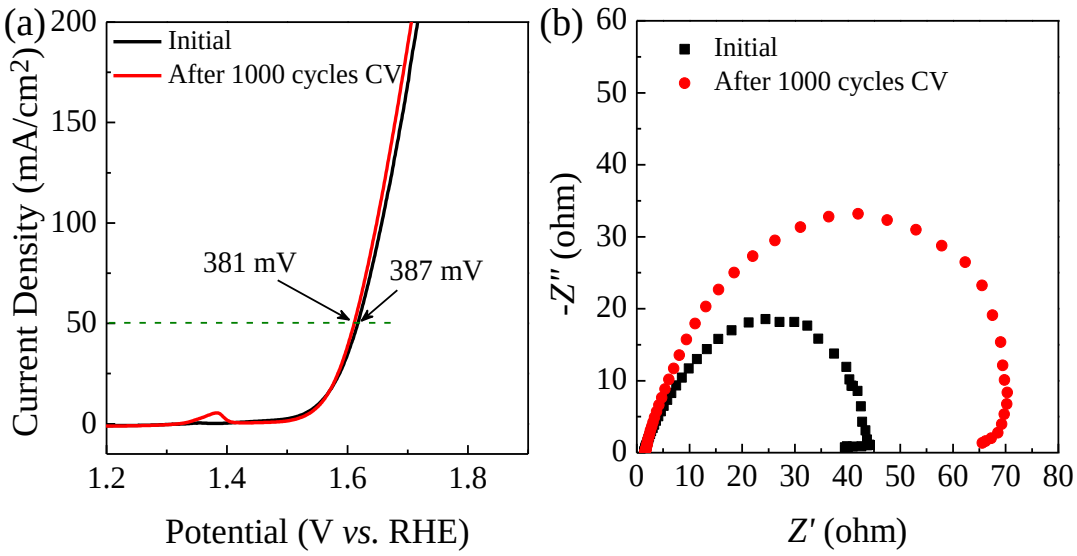

Fig. S14. Electrochemical testing of Fe-CoO while the immersion concentration is 0.1 M (a) LSV curves, (b) Nyquist plots with an initial and after 1000 cycles CV test.

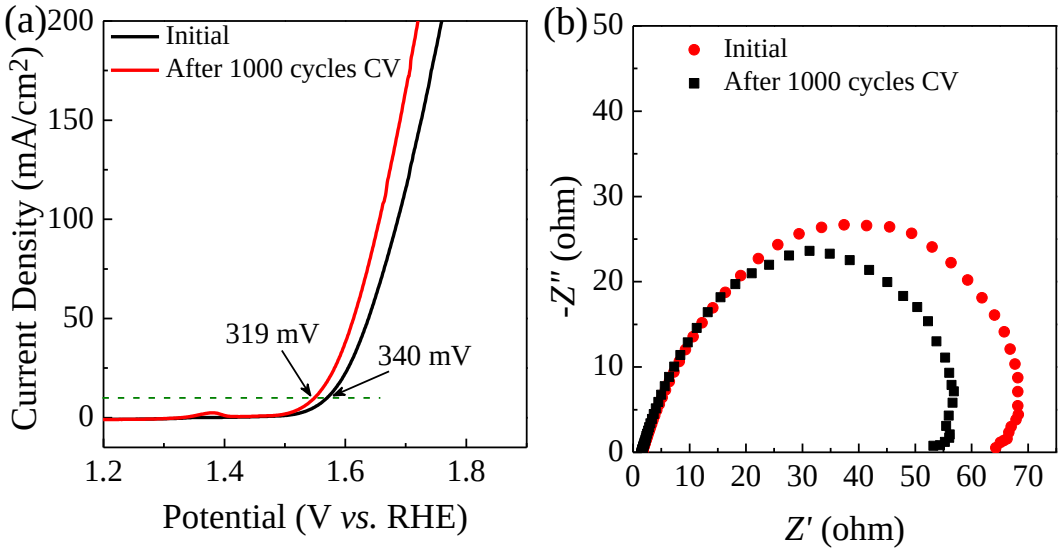

Fig. S15. Electrochemical testing of Fe-CoO while the immersion concentration is 0.03 M (a) LSV curves, (b) Nyquist plots with an initial and after 1000 cycles CV test.

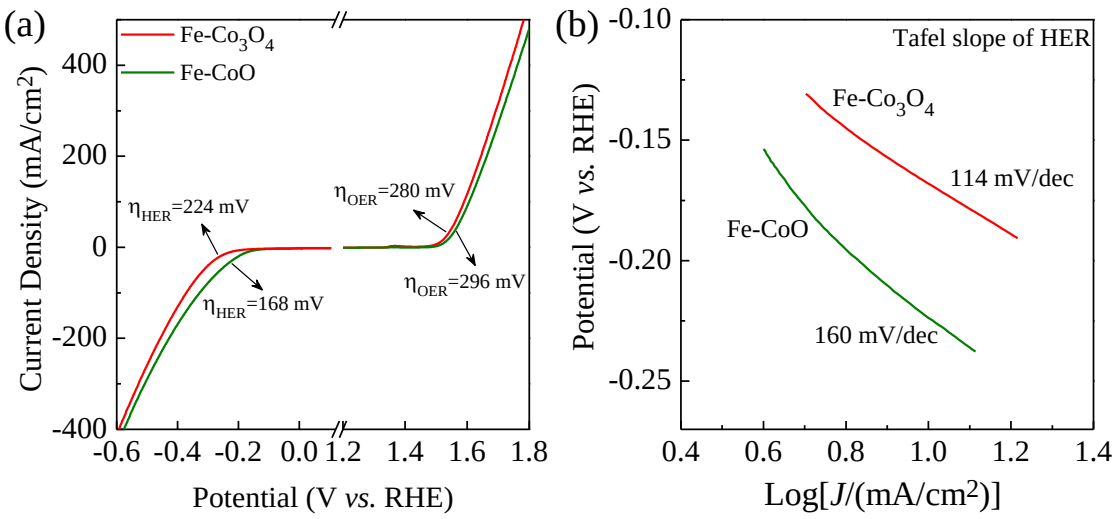

Fig. S16. (a) OER and HER curve of Fe-Co_3O_4 and Fe-CoO, (b) Tafel plots of Fe-Co_3O_4 and Fe-CoO.

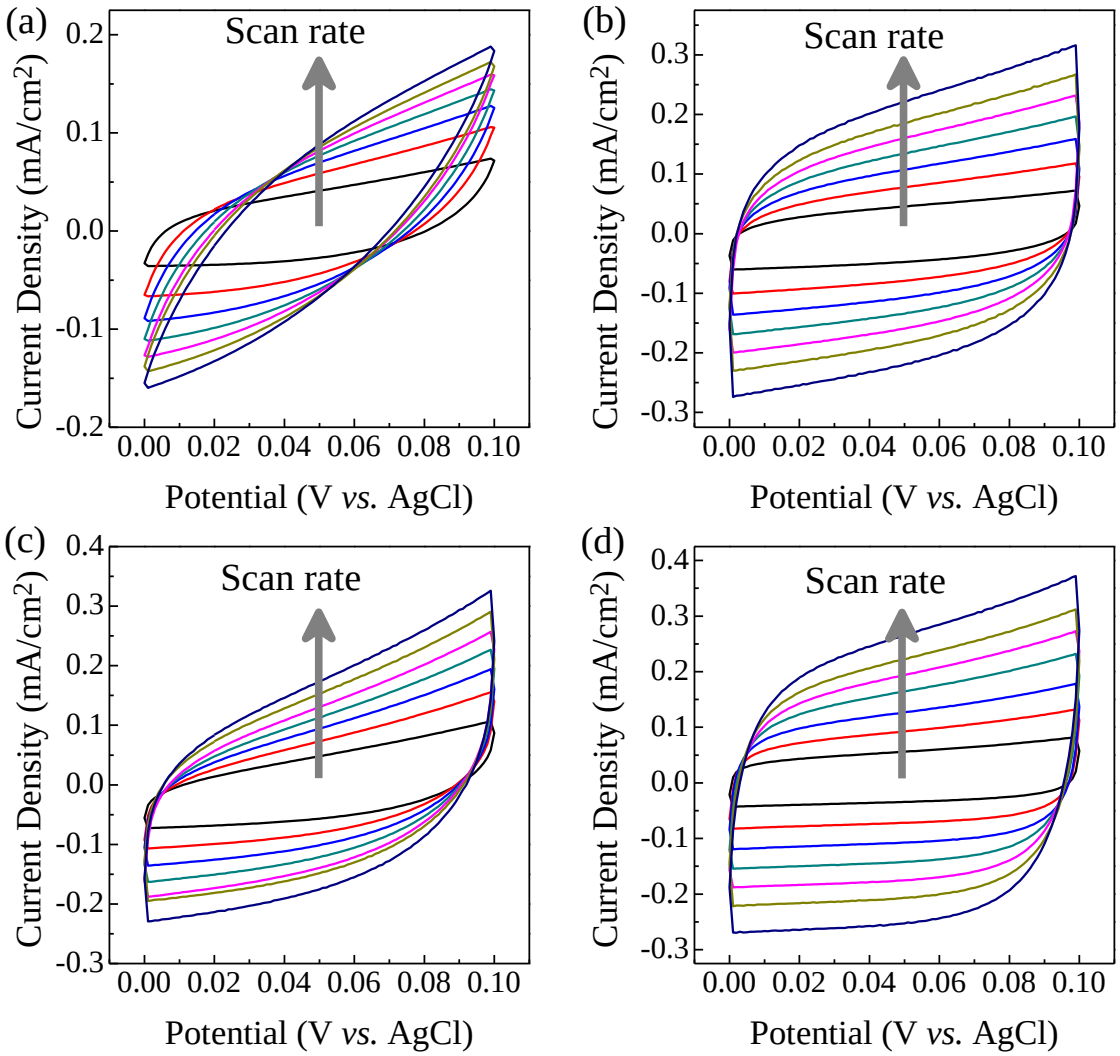

Fig. S17. CVs of Co_3O_4 (a), Fe-Co_3O_4 (b), CoO (c) and Fe-CoO (d) with increasing scan rates.

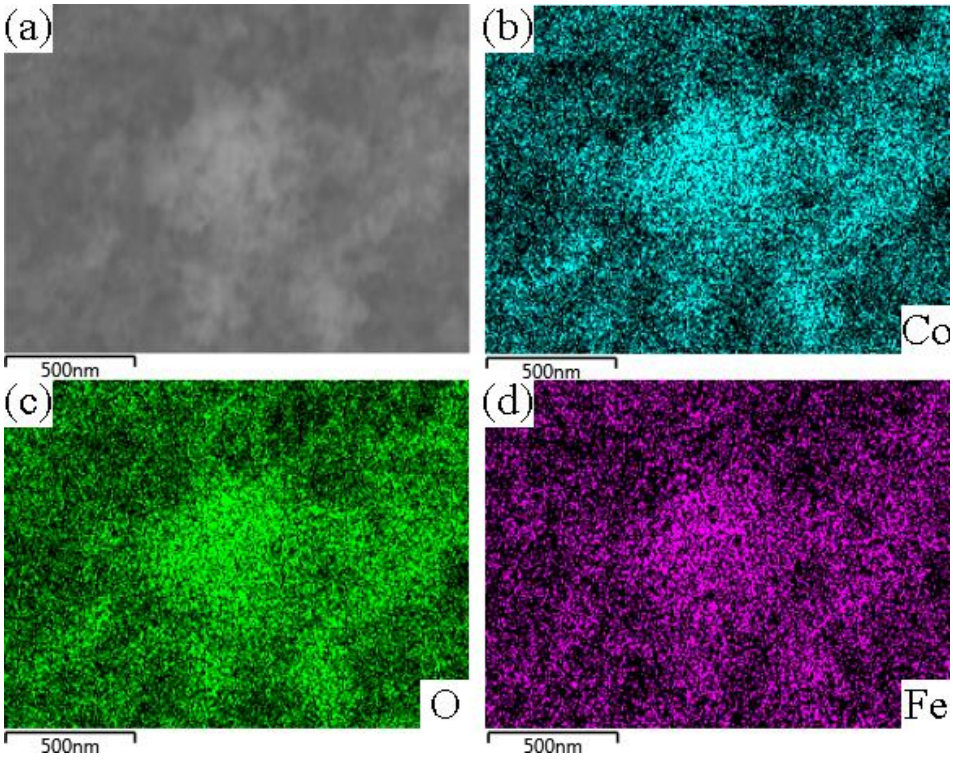

Fig. **S18.** SEM image (a), elemental mapping of Co (b), O (c) and Fe (d) element in Fe-Co_3O_4 after *i-t* test.

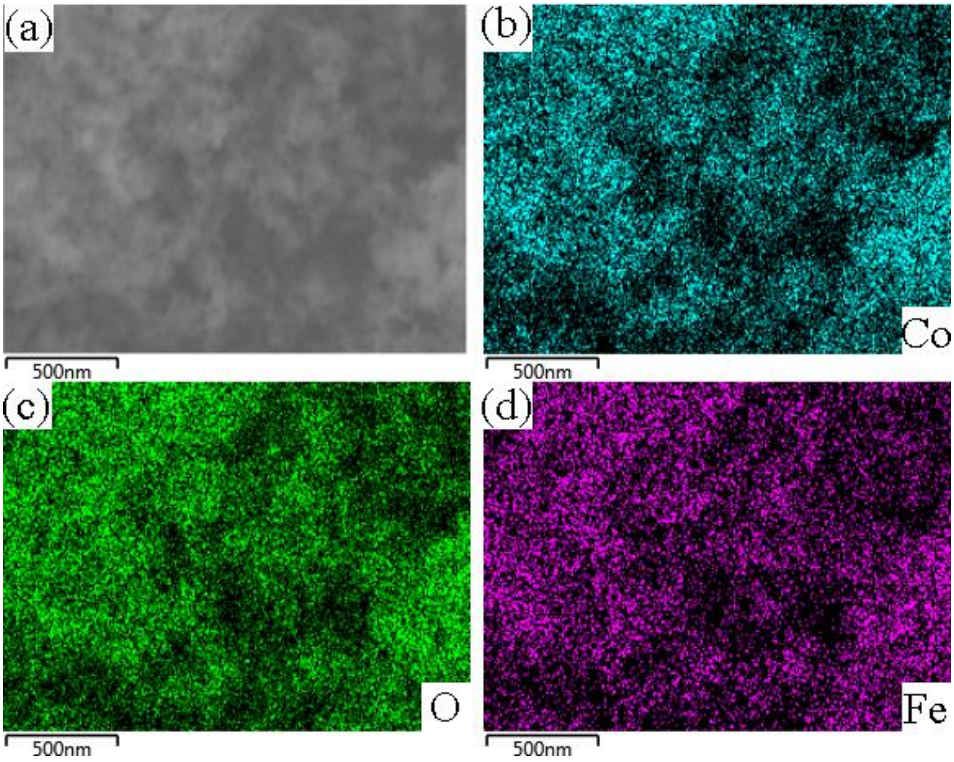

Fig. **S19.** SEM image (a), elemental mapping of Co (b), O (c) and Fe (d) element in Fe-CoO after *i-t* test.

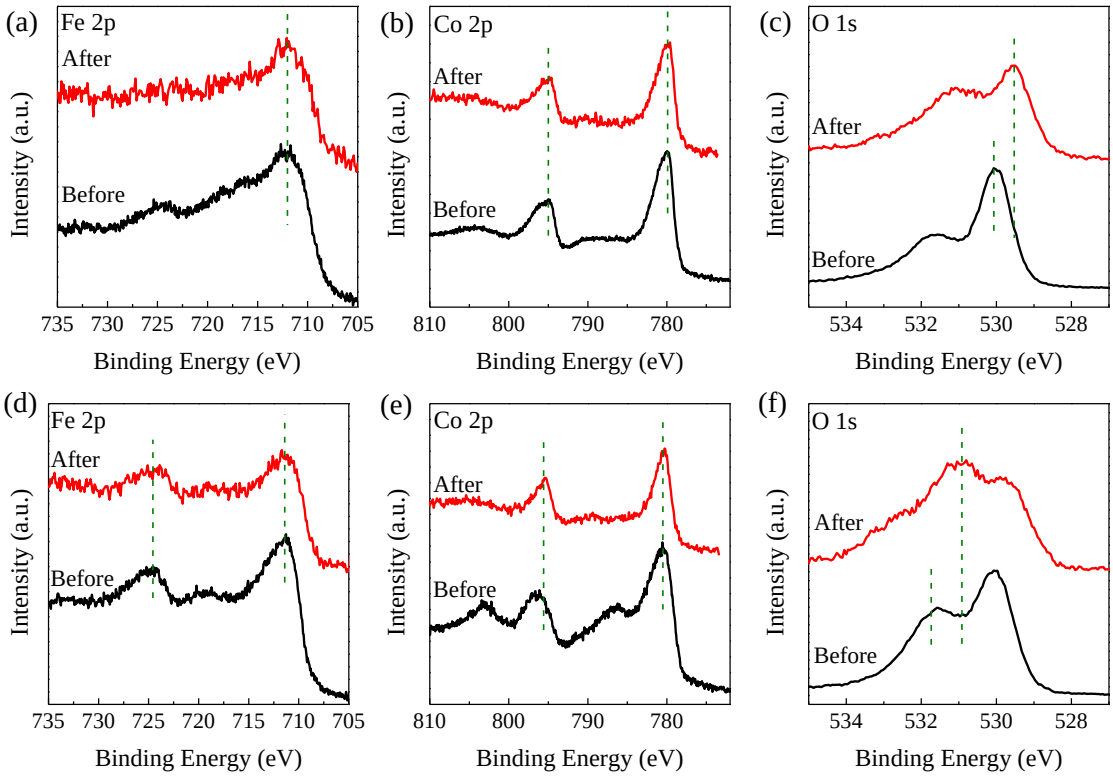

Fig. **S20**. High-resolution XPS spectrum of Fe 2p (a), Co 2p (b) and O 1s (c) for Fe-Co_3O_4 and Fe 2p (d), Co 2p (e) and O 1s (f) for Fe-CoO before (black line) and after (red line) *i-t* test.

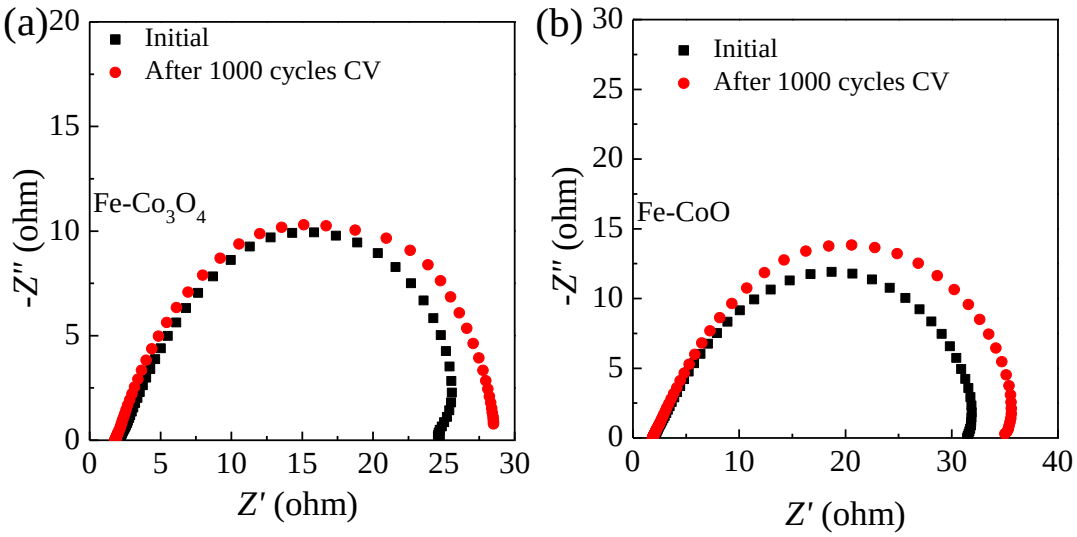

Fig. S21. Nyquist plots of Fe-Co_3O_4 (a) and Fe-CoO (b) for initial and after 1000 cycles CV test.

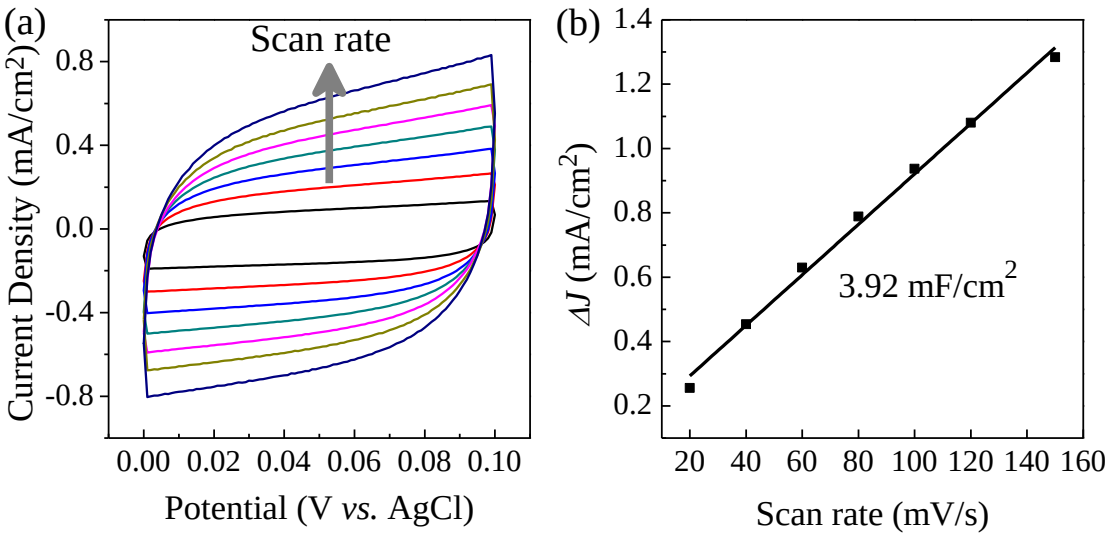

Fig. S22. (a) CV of Fe-Co_3O_4 with increasing scan rates after CV cycles (b) C_{dl} calculated value of Fe-Co_3O_4 after CV cycles.

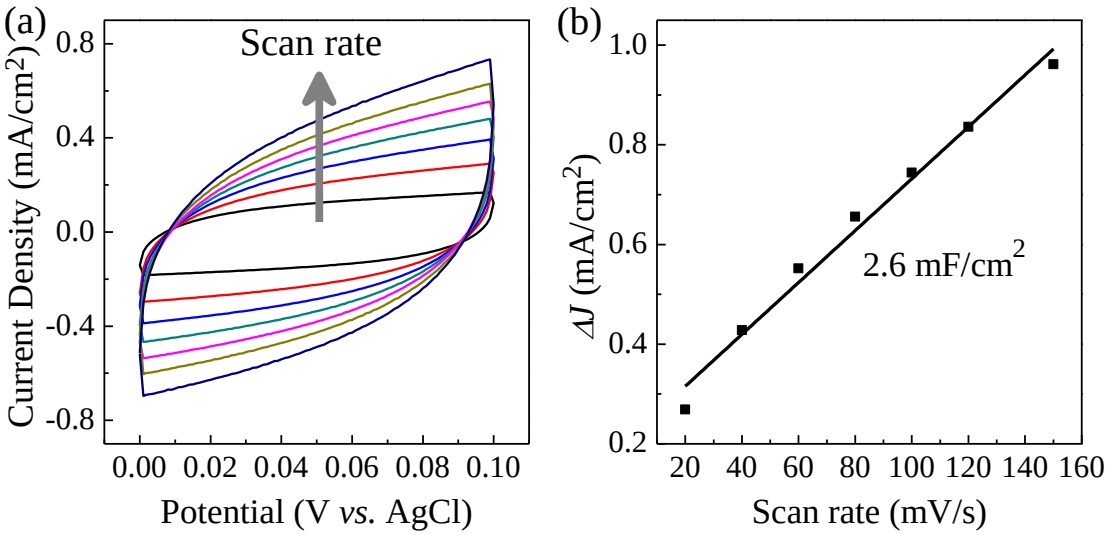

Fig. S23. (a) CV of Fe-CoO with increasing scan rates after 1000 CV cycles (b) C_{dl} calculated value of Fe-CoO after CV cycles.

Table S1 The electrocatalytic OER activity of Fe-Co_3O_4 by different Fe ion concentrations in soak solution

Fe ion concentrations in soak solution	Overpotential (mV)	Current density @1.8 V (mA/cm^2)	Charge transfer resistance (Ω)
0.01 M (Initial)	343 (10 mA/cm^2)	294	45.7
0.01 M (After 1000 CV)	326 (10 mA/cm^2)	296	62.5
0.02 M (Initial)	280 (10 mA/cm^2)	542	22.6
0.02 M (After 1000 CV)	263 (10 mA/cm^2)	597	26.6
0.03 M (Initial)	325 (10 mA/cm^2)	303	27.8
0.03 M (After 1000 CV)	314 (10 mA/cm^2)	349	43.8
0.04 M (Initial)	331 (10 mA/cm^2)	285	35.2
0.04 M (After 1000 CV)	323 (10 mA/cm^2)	303	60.4

Table S2 The electrocatalytic OER activity of Fe-CoO by different Fe ion concentrations in soak solution

Fe ion concentrations in soak solution	Overpotential (mV)	Current density @1.8 V (mA/cm^2)	Charge transfer resistance (Ω)
0.01 M (Initial)	387 (50 mA/cm^2)	365	41.9
0.01 M (After 1000 CV)	381 (50 mA/cm^2)	398	63.8
0.02 M (Initial)	296 (10 mA/cm^2)	480	29.6
0.02 M (After 1000 CV)	272 (10 mA/cm^2)	539	33.1
0.03 M (Initial)	340 (10 mA/cm^2)	269	51.4
0.03 M (After 1000 CV)	319 (10 mA/cm^2)	354	62.5

Table S3 Comparison of OER performance of some cobalt oxide based electrocatalysts in recently work.

Sample	Electrolyte	Current density (mA/cm^2)	η(mV)	Tafel slope (mV/dec)
Fe-Co_3O_4 (This work)	1 M KOH	10 mA/cm^2	280	55
Fe-CoO (This work)	1 M KOH	10 mA/cm^2	296	55
RuO_2 (This work)	1 M KOH	10 mA/cm^2	306	142
Co_3O_4-MWCNT[1]	1 M KOH	10 mA/cm^2	320	69
Co_3O_4-B[2]	1 M KOH	10 mA/cm^2	318	57.6
S-CoO/Co_3O_4[3]	1 M KOH	10 mA/cm^2	275	92
Hemoglobin modified Co_3O_4-g-C_3N_4[4]	0.5 M KOH	10 mA/cm^2	370	66
Co_3O_4 nanoflowers[5]	1 M KOH	10 mA/cm^2	297	79.1
Co_3O_4/CoO[6]	1 M KOH	10 mA/cm^2	302	68.6

References

1. X, Zhang, Y. S. Chen, P. V. Kamat, S Ptasinska, Probing Interfacial Electrochemistry on a Co_3O_4 Water Oxidation Catalyst Using Lab-Based Ambient Pressure X-Ray Photoelectron Spectroscopy. *J. Phys. Chem. C* 2018, **122**, 13894-13901.

2. R. Wei, M. Fang, G. Dong, C. Lan, L. Shu, H. Zhang, X. Bu, J. C. Ho, High-Index Faceted Porous Co_3O_4 Nanosheets with Oxygen Vacancies for Highly Efficient Water Oxidation. *ACS Appl. Mater. Interfaces* 2018, **10**, 7079-7086.

3. T. Sun, P. Liu, Y. Zhang, Z. Chen, C. Zhang, X. Guo, C. Ma, Y. Gao, S. Zhang, Boosting the Electrochemical Water Splitting on Co_3O_4 through Surface Decoration of Epitaxial S-Doped Coo Layers. *Chem. Eng. J.* 2020, **390**, 124591.

4. C. Leal-Rodriguez, D. Rodriguez-Padron, Z. A. Alothman, M. Cano, J. J. Giner-Casares, M. J. Munoz-Batista, S. M. Osman, R. Luque, Thermal and Light Irradiation Effects on the Electrocatalytic Performance of Hemoglobin Modified Co_3O_4-g-C_3N_4 Nanomaterials for the Oxygen Evolution Reaction. *Nanoscale* 2020, 12, 8477-8484.

5. J. Du, C. Li, Q. Tang, Oxygen Vacancies Enriched Co_3O_4 Nanoflowers with Single Layer Porous Structures for Water Splitting. *Electrochim. Acta* 2020, **331**, 135456.

6. Z. Liu, Z. Xiao, G. Luo, R. Chen, C. L. Dong, X. Chen, J. Cen, H. Yang, Y. Wang, D. Su, Y. Li, S. Wang, Defects-Induced in-Plane Heterophase in Cobalt Oxide Nanosheets for Oxygen Evolution Reaction. *Small* 2019, **15**, 1904903.